Research Article | Vol. 12, No. 9 / 1 Sep 2021 / Biomedical Optics Express 5583
Biomedical Optics EXPRESS

Treatment with LEDs at a wavelength of 642 nm enhances skin tumor proliferation in a mouse model

HYEYOON GOO,[1,2] SANGJOON MO,[2] HYEONG JU PARK,[2] MIN YOUNG LEE,[2,3,4,5,*] AND JIN-CHUL AHN[1,2,4,5]

[1]Department of Medical Laser, Graduate School of Medicine, Dankook University, Cheonan 31116, Republic of Korea
[2]Medical Laser Research Center, Dankook University, Cheonan 31116, Republic of Korea
[3]Department of Otolaryngology-Head & Neck Surgery, College of Medicine, Dankook University, Cheonan 31116, Republic of Korea
[4]Beckman Laser Institute Korea, Dankook University, Cheonan 31116, Republic of Korea
[5]Contributed equally
*eyeglass210@gmail.com

Abstract: Photobiomodulation (PBM) is attracting increased attention in the fields of dermatology and cosmetics. PBM with a variety of light parameters has been used widely in skin care, but can cause certain types of unwanted cells to proliferate in the skin; this can lead to skin tumors, such as papillomas and cancers. We constructed a mouse model of human skin tumors using DMBA as an initiator and TPA as a promoter, and confirmed that LEDs with a wavelength of 642 nm (red light) increased tumor size, epidermal thickness, and systemic proinflammatory cytokine levels. These results indicated that skin tumor cell proliferation may result from the use of 642 nm LEDs, suggesting the need for regulation of skin care based on LED light therapy.

1. Introduction

Photobiomodulation (PBM) near-infrared (NIR) light (600–1,000 nm) delivered from a laser or non-coherent light source, has been shown to have beneficial effects in a wide range of pathologies [1]. Numerous studies have confirmed the efficacy of PBM [2–7]. One medical application of PBM is the regulation of tumor cell growth [8–10]; however, several studies also reported proliferation of dysplastic lesions after PBM [11–13]. This may be related to the biphasic effects of medical light therapies: high light energy is used to regulate the abnormal growth of cells, while low light energy is used to induce proliferation or differentiation of target cells in tissues that are damaged or degenerated. However, if the light energy is delivered to the wrong target, such as tissue that has a tendency to form neoplastic lesions, unexpected outcomes may arise [11–13].

The skin, as the largest organ of the human body, is comprised of various layers, including the epidermis and dermis [14]. These layers are complex systems composed of numerous cell types, each of which has distinct optical properties [15,16]. PBM has attracted increasing attention in the fields of dermatology and cosmetics, and has been shown to be effective for improving the appearance of wrinkles and skin laxity [5,6,17–19]. PBM with a variety of light parameters, including red light, has been used widely in skin care, but can cause certain types of unwanted cells to proliferate in the skin; this can lead to skin tumors, such as papillomas and cancers. Several animal models of skin tumor development have been reported. For example, genetic changes are induced in mice by the application of 7,12-dimethylbenz(a)anthracene (DMBA) [20], and repeated application of 12-O-tetradecanoylphorbol-13-acetate (TPA) induces permanent mutation of cells [21].

#427205 https://doi.org/10.1364/BOE.427205
Journal © 2021 Received 9 Apr 2021; revised 30 Jul 2021; accepted 31 Jul 2021; published 13 Aug 2021

Biomedical Optics EXPRESS

Red laser light, which is part of the visible light spectrum, is capable of stimulating cell proliferation [11] and directly impacts the soft tissue of the skin dermis [22,23]. In the present study, we constructed a mouse model of human skin tumors using DMBA as an initiator and TPA as a promoter. Our observations confirmed that light-emitting diodes (LEDs) with an emission wavelength of 642 nm (red light) increased tumor volume, epidermal thickness, and systemic proinflammatory cytokine levels.

2. Materials and methods

2.1. Skin tumor mouse model

The study protocol was approved by the Dankook University Medical School Research Institutional Animal Care and Use Committee (DKU20-009). A total of 3 sets of experiments were performed. Six-to-seven-week-old female Crl:SKH1-hr hairless mice and ICR mouse were purchased from the LAB animal center (Republic of Korea). The mice were randomly divided into three groups (Control, DMBA/TPA, DMBA/TPA + LED). The experimental design of the in vivo study is outlined in Fig. 1(a). Briefly, the backs of the mice were shaved and 60 μg of DMBA (9,10-dimethylbenz[a]anthracene; Sigma, St. Louis, MO, USA) dissolved in 0.2 mL of acetone was applied to the naked dorsal skin in the DMBA/TPA and DMBA/TPA + LED groups. Two weeks after skin tumor initiation with DMBA, animals in the DMBA/TPA and DMBA/TPA + LED groups were further exposed to 4 μg/0.2 mL of TPA (12-O-tetradecanolyphorbal-13-acetate; Sigma) twice a week for a total of 20 weeks (from week 3 to week 22). In addition, Acetone only and acetone + LED groups were included as control groups. The body weights of animals were recorded at baseline, and once per week thereafter. Tumors appearing on the skin were evaluated every week during the experimental period.

2.2. LED treatment

An array of 126 LEDs with an emission wavelength of 642 nm (WonTech Co. Ltd., Seoul, Republic of Korea) was used in this study. Mouse tissue temperature was measured before and after 30 min of treatment, respectively. Temperatures were measured using a Fluke 62 Mini Infrared IR Thermometer (accuracy; ±1.5%), and all groups treated with LEDs were performed. As a result, there was no significant difference between 34.4 ± 0.9°C before treatment and 34.2 ± 1.1°C after treatment. This is because a fan was used to prevent excessive heat generation while curing the LED. The light source for irradiating the surface of the mouse skin used LED (CL-SFC506USD, Ciel Light) module and a 0.2 W intensity LED chip. LEDs were used by arranging a total of 126 (14×9) on a PCB of 14.6×21.0 cm. The power of the LED panel was supplied by power-supply (GPS-2303, GW Instek), 19.5 V (642 nm LED), and used according to the same power intensity as the photodiode power-meter (PD300-TP-ROHS, Ophir Optronics). The energy at the bottom of the plate was measured with a laser power meter. The mice were irradiated twice a week with LEDs at 642 nm after each DMBA/TPA treatment. A power of 12 mW/cm^2 was delivered for 30 min, resulting in a total fluence of 21.6 J/cm^2 for one LED treatment (Fig. 1). The distance between the LED panel and the mouse dorsal skin is 5 cm, and an area of 5 points among 4×2 cm dorsal skin was randomly designated and treatment was measured. As a result, averaged power level was measured as 11.99 ± 0.07 mW/cm^2. Variation of LED treatment on the mouse dorsal skin were minimal (11.9, 12.0, 12.1, 11.95, 12.0 mW/cm^2). In addition, spectrometer analysis of DMBA, TPA, and acetone that dissolves DMBA and TPA using a (UV-1650, SHIMADZU, Kyoto, Japan) was performed. Detailed information on the laser parameters, including the full-width at half-maximum and electrical power of the LEDs, is presented in Table 1.

Biomedical Optics EXPRESS

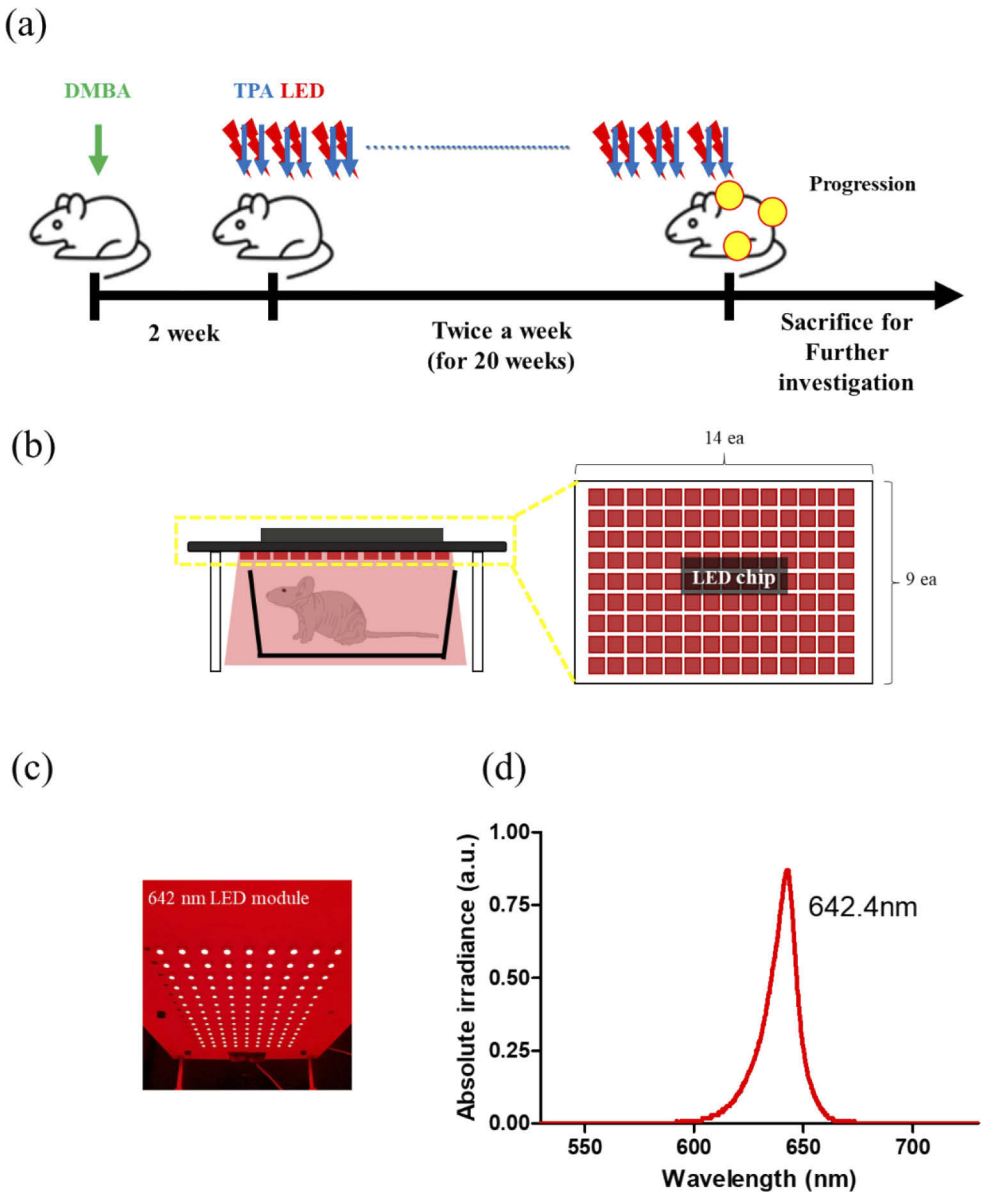

Fig. 1. Experimental schedule and LED spectrum (a) Female SKH-1 hairless mice aged 6 weeks were used. To initiate tumor development, DMBA was applied to the dorsal skin. Two weeks after DMBA application, LED treatment (21.6 J/cm^2) was applied immediately after TPA application to the DMBA-treated area. All procedures were performed twice a week for 20 weeks. (b) The light source panel for irradiating the mouse was used by 126 chips, (c) 642 nm LED module (d) LED treatment spectrum with an emission wavelength of 642 nm.

Biomedical Optics EXPRESS

Table 1. LED Device information and Parameters[a]

Treatment wavelength (nm)	642 nm
Manufacturer	Wontech Co. Ltd., ROK
Light type	Light-emitting diode
Number of array	126 (14 × 9)
Mode	Continuous wave (CW)
FWHM	TYP 16.8 nm/LED
Treatment time	30 min
Total fluence	21.6 J/cm^2

[a]Abbreviations: FWHM, full-width-half-maximum

2.3. Epidermal thickness in H&E staining

The tissues were fixed in a 10% neutral buffered formalin and dehydrated with xylene and a gradient alcohol series. Samples were embedded in paraffin blocks and cut into 5-μm-thick sections using a microtome. The sections were stained in Harris hematoxylin solution for 5 min and then differentiated in 1% acid alcohol after deparaffinization. The sections were rinsed with tap water and counterstained in eosin Y solution for 2 min. The sections were observed under a microscope (BX53; Olympus, Tokyo, Japan) at the Center for Bio-medical Engineering Core Facility (Dankook University, Korea) and photographed after mounting. The epidermal thickness of hematoxylin and eosin (H&E)-stained sections was assessed using Image J software (NIH, Bethesda, MD, USA).

2.4. Collagen staining in Picro-sirius red staining

Picrosirius red staining was performed according to the standard protocol. Briefly, sections were stained with Harris' hematoxylin for 10 min. After washing with tap water for 10 min, the sections were stained with Picrosirius red for 1 h. The sections were further rinsed in two changes of acidified water, after which most of the water was physically removed from the slides by vigorous shaking followed by dehydration in three changes of 100% ethanol. Finally, sections were cleared in xylene and mounted. Under microscopic observation, collagen appears red on a pale yellow background with Picrosirius red staining. Quantification of the collagen fibers was performed with Image J software.

2.5. Immunohistochemistry

For immunohistochemical analysis, the sections were washed twice with 1× PBS for 5 min each time, and then blocked by incubation with 5% BSA dissolved in 1× PBS for 1 hour. The sections were then incubated with primary antibody to interleukin (IL)-1β, IL-6, or tumor necrosis factor (TNF)-α overnight at 4°C. The next day, sections were washed twice for 5 min each time in 1× PBS, and then incubated with biotinylated secondary antibody for 1 h at room temperature. Sections were then treated with ABC solution (Vectastain ABC Elite kit; Vector Laboratories) for 1 h, and washed with 1× PBS and 3,3′-diaminobenzidine (DAB) peroxidase substrate (Vector Laboratories) for 2 min. Counterstaining was carried out using Harris' hematoxylin for 20 sec. Stained sections were viewed under a microscope, and the processed images were analyzed using Image J software.

2.6. Serum cytokine levels

Cytokine levels in serum were determined using mouse IL-1β, IL-6, and TNF-α enzyme-linked immunosorbent assay (ELISA) kits (Quantikine; R&D Systems, Minneapolis, MN, USA) in

Biomedical Optics EXPRESS

accordance with the manufacturer's protocol. Briefly, for IL-1β, IL-6, and TNF-α kits, 100 µL of standard and samples were incubated on antibody-coated plates for 2 h. After washing three times, 100 µL of TMB substrate solution was added and plates were incubated at 37°C in the dark. Then, 100 µL of stop solution was added and the absorbance at 450 nm (A_{450}) was read on a microplate reader within 30 min.

2.7. Statistical analysis

All data from experimental are expressed as the mean ± standard deviation of the mean (SEM). All data were analyzed using GraphPad Prism (GraphPad Software, La Jolla, CA, USA) or Chi square calculator (https://www.graphpad.com/quickcalcs/chisquared1). Shapiro-Wilk normality tests were used to determine whether the data were parametric of nonparametric. In case of comparison between two groups, the *t*-test (parametric) and Man Whitney U-test (non-parametric) were used. In case of comparison among groups (>2), to reject the null hypothesis, estimation of the one-way analysis of variance (ANOVA) with Dunn's Multiple Comparison test and two-way ANOVA with Bonferroni post hoc analysis were used. $p < 0.05$ was considered statistically significant and was also defined as $*p < 0.05$, $**p < 0.01$ and $***p < 0.001$.

3. Result

3.1. Effect of LED treatment on DMBA/TPA-induced mouse skin tumorigenesis

TPA treatment was performed 2 weeks after DMBA treatment in female hairless mice. TPA treatment was performed twice a week, followed by LED treatment. At the end of the 22 weeks experimental period, no papillomas were seen on the dorsal skin in the control group. However, several papillomas were detected in the DMBA/TPA group, and several papillomas merged to form large papillomas in the DMBA/TPA + LED group (Suppl. Fig. 1) (Fig. 2(a)). The mice in all treatment groups showed no substantial changes in body weight, diet, or water consumption during the experimental period. The body weight of mice was measured weekly after the start of the experiment, and no significant group differences were detected (Fig. 2(b)). At 6 weeks after starting TPA treatment, tumors began to develop on the dorsal skin. The tumor incidence was ≥ 80% in the DMBA/TPA group and DMBA/TPA + LED groups (Fig. 2(c)). The average number of tumors increased over time in both the DMBA/TPA and DMBA/TPA + LED groups, and significantly from the control group from 16 weeks. In addition, the number of tumors began to develop more in the DMBA/TPA + LED group than in the DMBA/TPA group, and a significant difference was demonstrated at 16 weeks and 17 weeks (Fig. 2(d)) (two-way ANOVA; $p < 0.0001$; statistical significance after Bonferroni post hoc analysis is shown as $* p < 0.05$, $** p < 0.01$ compared with Control group and $^{\dagger} p < 0.05$, $^{\dagger\dagger} p < 0.01$ compared with DMBA/TPA group) (Table 2). To investigate this further, the tumors were categorized according to size at 20 weeks in each group. The results indicated that small tumors (0 to 1 mm), while tumors diameter 1 to <2, 2 to < 3 and > 3 mm were more prevalent in the DMBA/TPA + LED group than the DMBA/TPA group (Chi-square test; 45.0535, $p < 0.05$) (Fig. 2(e)). Total tumor area per each animal were measured and compared between DMBA/TPA and DMBA/TPA + LED group. The averaged total tumor area of DMBA/TPA + LED group was statistically larger than that of DMBA/TPA group (two-tailed t-test; $**p < 0.0145$, p=0.0053; t=2.955; df=38) (Suppl. Fig. 2). A total of 3 sets of experiments were performed. Additional information on the two sets of experiments including control group (acetone only and acetone + LED which did not develop tumor formation) are included as Supplementary Figure 3 and Supplementary Table 1.

3.2. Effect of LED treatment on DMBA/TPA-induced skin epidermal thickness

After the experiment was completed, paraffin-embedded sections of the dorsal skin around tumorigenic mice were subjected to histological analysis. Persistent TPA stimulation can promote

Biomedical Optics EXPRESS

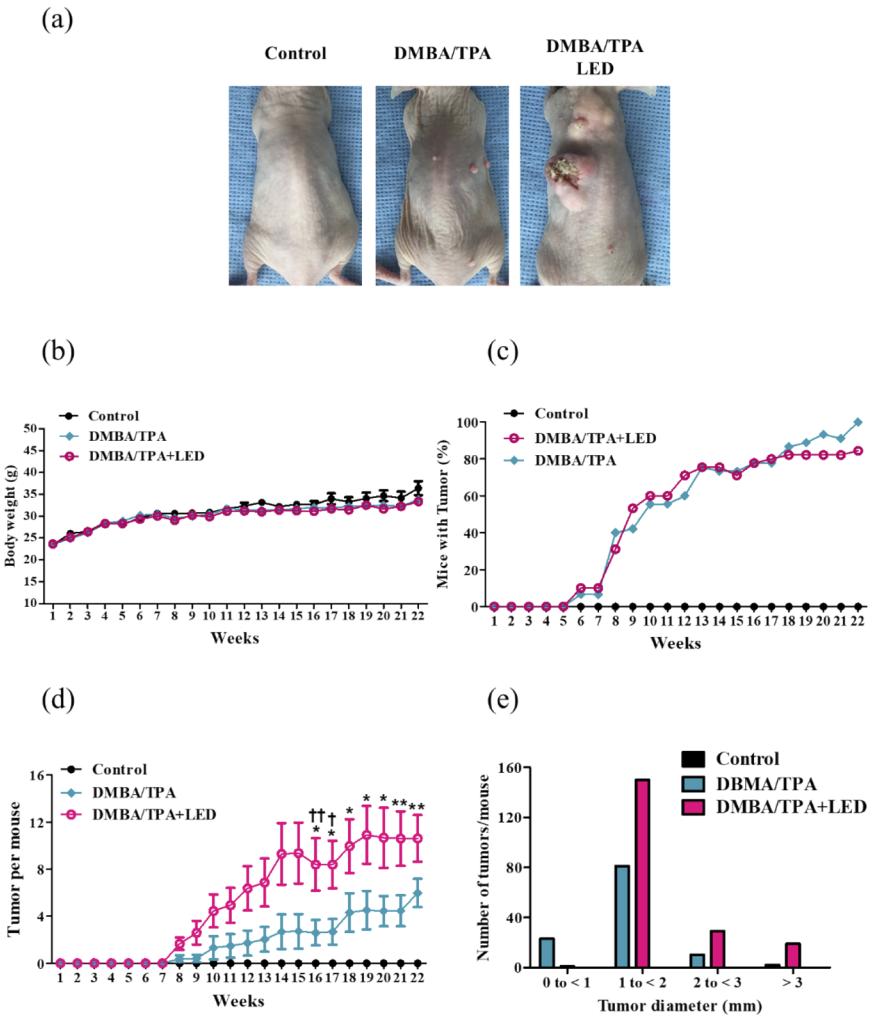

Fig. 2. LED treatment at 642 nm promoted tumor growth in the DMBA/TPA-induced mouse tumorigenesis model. The animals were divided into control (n=9), DMBA/TPA (n=25), and DMBA/TPA+LED groups (n=30). (a) At the end of the 22-week experiment, representative images of mice in each group. The control group showed no papilloma growth. The DMBA/TPA group showed several small papillomas in the dorsal area. In the DMBA/TPA+LED group, the papillomas showed increased size and several papillomas merged to form larger tumors. (b) The body weight of mice was measured weekly after the start of the experiment. There were no differences in body weight among the groups. (c) The tumor incidence (i.e., percentage of mice with tumors) was calculated. The DMBA/TPA and DMBA/TPA+LED groups showed significantly higher papilloma incidence rates compared to the control group. (d) The change in tumor multiplicity (i.e., average number of tumors) over time was assessed. The average number of tumors was significantly higher in the DMBA/TPA than control group, and was also significantly higher in the DMBA/TPA+LED group compared to the DMBA/TPA group. (e) The average number of tumors in each group. The tumor diameter was classified as 0–1 mm, 1–2 mm, 2-3mm and >3mm. The number of tumors 1-2mm, 2-3mm and >3mm were higher in the DMBA/TPA+LED group compared to the DMBA/TPA group. Error bars indicate standard deviation. *$p < 0.05$, ** $p < 0.01$ compared with Control group and † $p < 0.05$, †† $p < 0.01$ compared with DMBA/TPA group

Biomedical Optics EXPRESS

Table 2. Statistical Analysis of tumor per mouse results of 630 nm LED irradiation on DMBA/TPA-induced muse skin tumorigenesis[a]

Group	Control vs. DMBA/TPA	Control vs. DMBA/TPA+LED	DMBA/TPA vs. DMBA/TPA+LED
Two-way ANOVA (p Value)	***p<0.001	***p<0.001	***p<0.001
1-15W	ns	ns	ns
16W	ns	*	**
17W	ns	*	*
18W	ns	*	ns
19W	ns	*	ns
20W	ns	*	ns
21W	ns	**	ns
22W	ns	**	ns

[a]W, weeks.

skin epidermal thickening and infiltration of skin tumors [24]. H&E staining was performed to measure the epidermal thickness. Mice treated with DMBA/TPA showed epidermal proliferation with invasion of epidermal cells. In comparison to the control group, the thickness of the epidermis was significantly increased in the DMBA/TPA group (one-way ANOVA; P <0.0001; statistical significance after Dunn's Multiple Comparison test is shown as $***p < 0.001$), and the epidermis was significantly thicker in the DMBA/TPA + LED group compared to the other two groups (both, $***p < 0.001$). These observations suggested that LED treatment promotes epidermal thickening by increasing the tumor size (Fig. 3.).

3.3. Effect of LED treatment on DMBA/TPA-induced changes in collagen of skin

Collagen in the tissue stroma is an important factor in tumorigenesis. Extracellular matrix (ECM) is a major constituent of all tissues, and the main ECM protein is collagen [25]. Healthy tissues maintain their function through continuous ECM remodeling. However, when a tumor occurs, the function of the ECM is lost. Cancer cells secrete large amounts of matrix metalloproteinases (MMPs) that degrade collagen and reduce the amount of ECM [26]. After the experiment was completed, paraffin-embedded sections of the dorsal skin around tumor were subjected to collagen level analysis. In this study, the collagen content was measured by calculating the intensity of Picrosirius red staining in different areas of the images.

The results confirmed that the amount of collagen was significantly reduced in the DMBA/TPA group and DMBA/TPA + LED group compared to the control group. DMBA/TPA treatment has been shown to degrade collagen and decrease the amount of ECM. Moreover, When the LED was irradiated, it was confirmed that it reduced more than the DMBA/TPA group, but there was no significant difference. (one-way ANOVA; P = 0.0022; statistical significance after Dunn's Multiple Comparison test is shown as $**p < 0.01$) (Fig. 4.).

3.4. DMBA/TPA-induced activation of inflammatory cytokines in mouse skin

Immunohistochemical analysis was performed to confirm the inflammatory reaction in the dorsal skin. In each image area, positive expression of proinflammatory cytokines indicated by DAB staining was calculated using Image J. As shown in Fig. 5, the skin tissue was stained with DAB, and proinflammatory cytokines were highly expressed in the epidermis. Compared to the control group, the DMBA/TPA + LED group showed significantly increased TNF-α and IL-1β expression (one-way ANOVA; P = 0.0101; statistical significance after Dunn's Multiple Comparison test is shown as $*p < 0.5$, $***p < 0.001$). The expression levels of all proinflammatory cytokines

Biomedical Optics EXPRESS

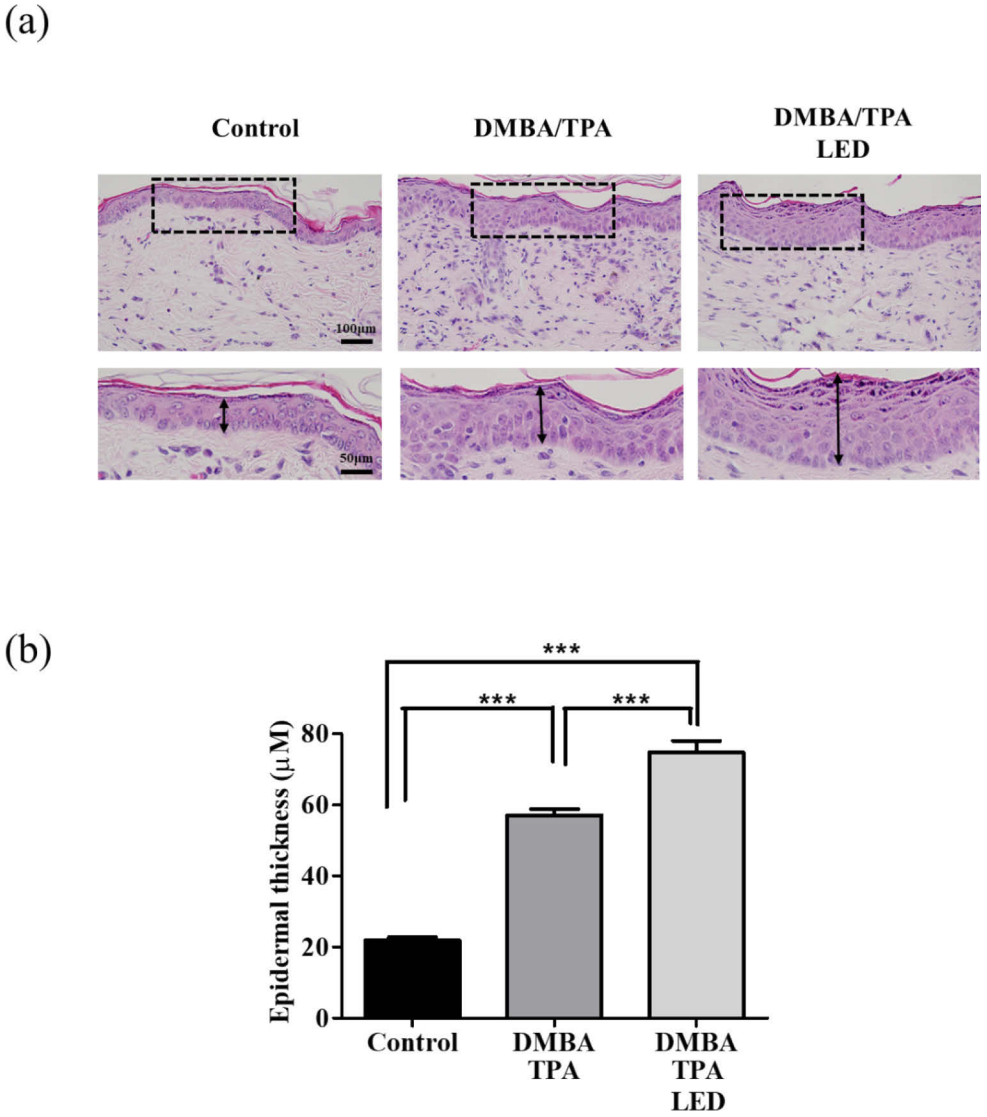

Fig. 3. LED treatment at 642 nm increased epidermal thickness in the DMBA/TPA-induced mouse tumorigenesis model. The animals were divided into control (n=9), DMBA/TPA (n=25), and DMBA/TPA+LED groups (n=30). (a) Representative images were showing epidermal proliferation (bidirectional arrow) in control, DMBA/TPA and DMBA/TPA+LED groups (H&E staining). Epidermal thickening of the dorsal skin was observed in the DMBA/TPA and DMBA/TPA+LED groups. The DMBA/TPA+LED group showed greater epidermal thickening compared to the DMBA/TPA group. Black arrow, epidermal thickness. (b) Quantitative analysis revealed significantly increased epidermal thickness in the DMBA/TPA+LED group compared to the DMBA/TPA and control groups. Black dotted square: location of the magnified figures below. Scale bars are indicated in each image. Error bars indicate standard deviation. $***p < 0.001$.

Biomedical Optics EXPRESS

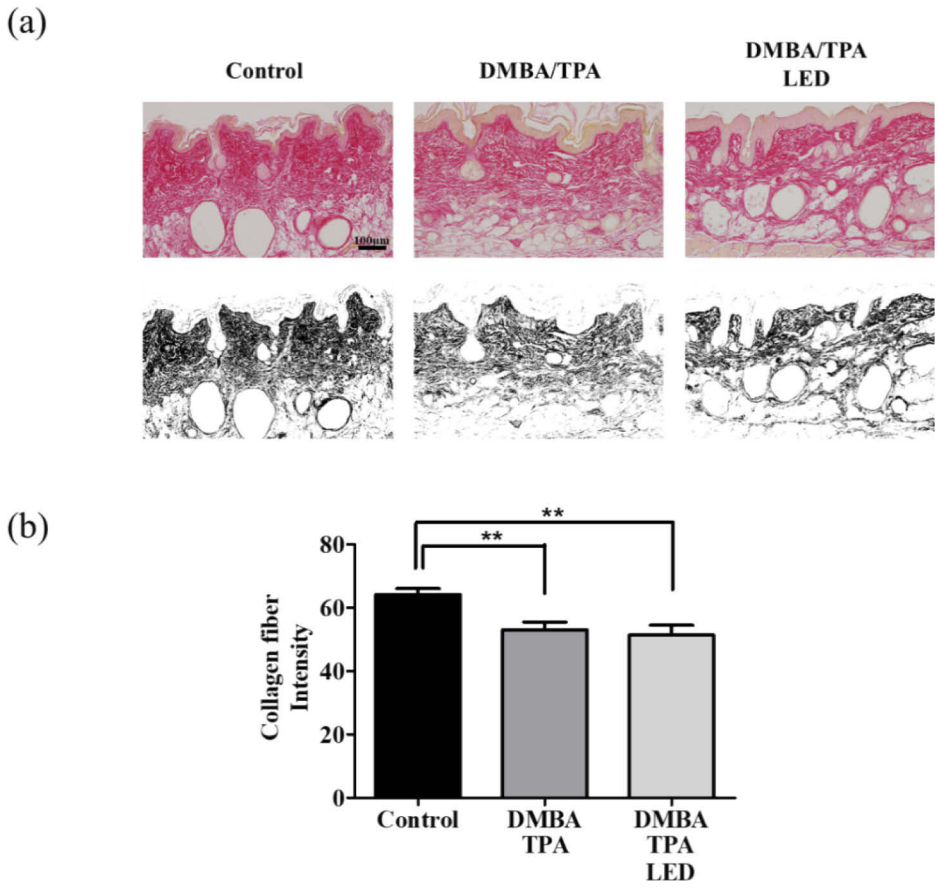

Fig. 4. Effect of 642 nm LED treatment on collagen level in the DMBA/TPA-induced mouse tumorigenesis model. The animals were divided into control (n=9), DMBA/TPA (n=25), and DMBA/TPA+LED groups (n=30). (a) Representative images showing collagen fiber staining intensity (Picrosirius red staining). The DMBA/TPA and DMBA/TPA+LED groups showed reduced collagen staining intensity compared to the control group. Moreover, the DMBA/TPA+LED group showed a greater decrease in collagen staining intensity compared to the DMBA/TPA group. (b) Quantitative analysis revealed significantly decreased collagen fiber staining intensity in the DMBA/TPA+LED group compared to the other groups. Error bars indicate standard deviation. $^{**}p < 0.01$. Scale bars, 100 μm

Biomedical Optics EXPRESS

examined were increased in the DMBA/TPA + LED group compared to the DMBA/TPA group, but the differences were not significant (Fig. 5).

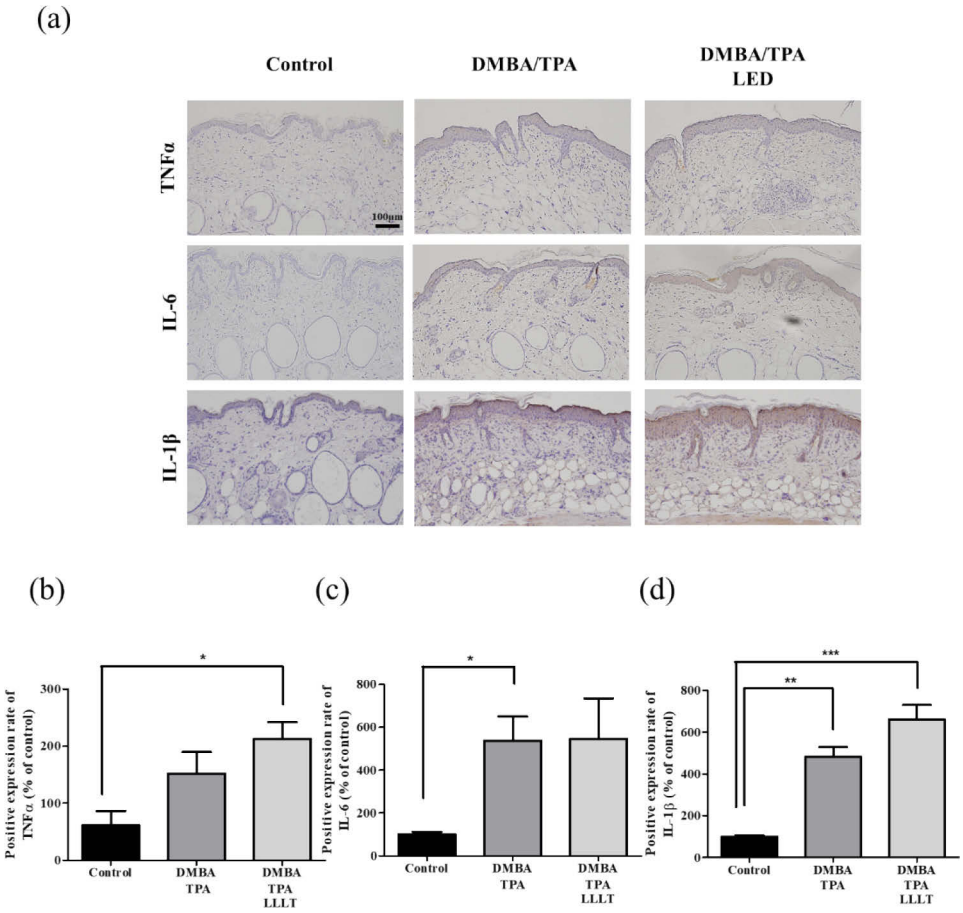

Fig. 5. Immunohistochemical analysis of proinflammatory cytokines in the DMBA/TPA-induced mouse tumorigenesis model. The animals were divided into control (n=9), DMBA/TPA (n=25), and DMBA/TPA+LED groups (n=30). The levels of the proinflammatory cytokines TNF-α, IL-6, and IL-β were determined by immunohistochemical analysis in DMBA/TPA-induced mice exposed to LED treatment. (a) Representative image of proinflammatory cytokine expression. (b) Quantitative analysis revealed increased TNF-α expression in the DMBA/TPA+LED group compared to the control group. (c) Quantitative analysis revealed increased IL-6 expression in the DMBA/TPA group compared to the control group. Although not significant, the level of IL-6 was expression was increased in the DMBA/TPA+LED group compared to the DMBA/TPA group. (d) IL-1β expression was increased in the DMBA/TPA and DMBA/TPA+LED groups compared to the control group, but there was no significant difference between the DMBA/TPA and DMBA/TPA+LED groups. Error bars indicate standard deviation. *$p < 0.5$, **$p < 0.01$ and ***$p < 0.001$ Scale bars, 100 μm.

3.5. *Effect of LED treatment on DMBA/TPA-induced systemic proinflammatory cytokines*

The serum of all groups was subjected to ELISA to examine systemic proinflammatory cytokine expression levels. The levels of IL-6 and TNF-α were different from those in the skin.

Biomedical Optics EXPRESS

The serum levels of IL-6 were significantly increased in the DMBA/TPA + LED groups compared to the control group (one-way ANOVA; P <0.0001; statistical significance after Dunn's Multiple Comparison test is shown as ***$p < 0.001$). In addition, the serum IL-6 level was significantly increased in the DMBA/TPA + LED group compared to the DMBA/TPA group (one-way ANOVA; P <0.0001; statistical significance after Dunn's Multiple Comparison test is shown as **$p < 0.01$). There was no significant difference in TNF-α expression in the DMBA/TPA and DMBA/TPA + LED groups compared to the control group. However, compared to the DMBA/TPA group, TNF-α expression was significantly increased in the DMBA/TPA + LED group (one-way ANOVA; P = 0.0334; statistical significance after Dunn's Multiple Comparison test is shown as *$p < 0.05$). (Figure 6).

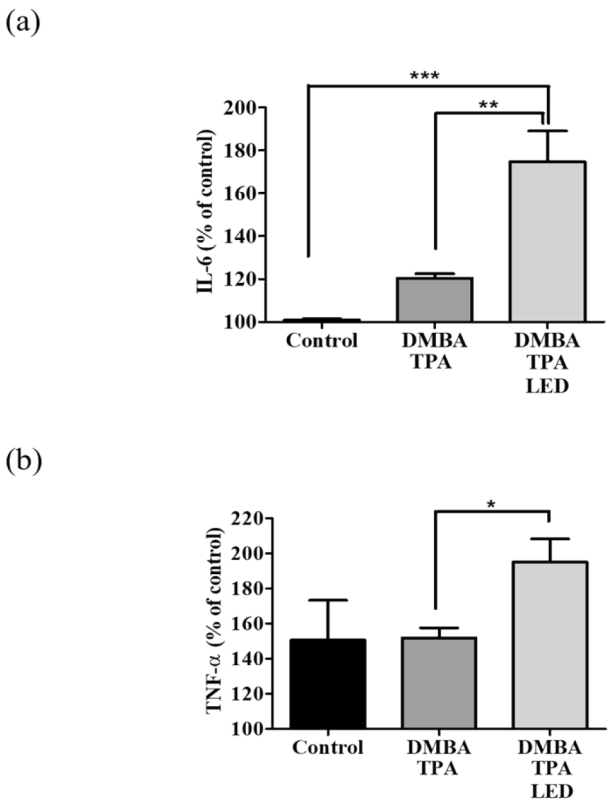

Fig. 6. Effect of 642 nm LED treatment on serum proinflammatory cytokine levels in the DMBA/TPA-induced mouse tumorigenesis model. The animals were divided into control (n=9), DMBA/TPA (n=25), and DMBA/TPA+LED groups (n=30). The levels of proinflammatory cytokines were determined by immunohistochemical analysis in DMBA/TPA-induced mice exposed to LED treatment. The levels of circulating IL-6 and TNF-α were evaluated by ELISA. (a) The serum IL-6 level was higher in the DMBA/TPA and DMBA/TPA+LED groups than the control group. Moreover, IL-6 expression was significantly higher in the DMBA/TPA+LED group than the DMBA/TPA group. (b) TNF-α expression was also elevated in the DMBA/TPA+LED group compared to the DMBA/TPA group. Error bars indicate standard deviation. *p < 0.05, **p < 0.01, ***p < 0.001.

4. Discussion

This study examined the effects of treatment with LEDs with an emission wavelength of 642 nm in the initiation stage of tumorigenesis. TPA treatment and LED treatment were performed from

Biomedical Optics EXPRESS

2 weeks after DMBA treatment. Tumors developed after 6 weeks of TPA treatment. In the LED treatment group, we confirmed that LEDs with an emission wavelength of 642 nm (red light) increased tumor diameter, epidermal thickness, and systemic proinflammatory cytokine levels. Therefore, the possibility that malignant transformation of these tumors was catalyzed by LED treatment should not be discounted.

The two-stage model of skin tumorigenesis induced by DMBA/TPA in hairless mice is an excellent vivo model, and can be used to investigate the multistep process of tumorigenesis, including initiation, promotion, and progression. DMBA was repeatedly applied to mouse skin to induce skin lesions, resulting in the transformation of normal cells into cancer cells [27]. TPA promotes tumor formation by ascending production [28].

The majority of previous reports on the effects of light energy on tumorigenesis indicated an inhibitory effect on tumor formation. Therefore, methods for delivering light energy, such as laser therapy, have been used in the clinical setting to treat malignancies in the larynx, cervix, etc. However, LED treatment can have both stimulatory and inhibitory effects on tumor cell proliferation [11]. The stimulatory effects of LED treatment have been investigated in tumor cells [29]. For example, Kreisler and AiHaj [30] reported that LED treatment promoted the proliferation of epithelial tumor cells in vitro. Similarly, Wernect et al. reported an increase in proliferation of Hep2 cells after LED treatment with emission wavelengths of 685 and 830 nm [31]. Furthermore, the results of the present study demonstrated that LED treatment markedly increased tumor size, epidermal thickness, and serum proinflammatory cytokine levels.

In this study, we observed increased proinflammatory cytokine levels in tumor tissue associated with the application of DMBA/TPA. We also demonstrated increased systemic proinflammatory cytokine levels after LED treatment compared to DMBA/TPA only. These two contradictory results will now be discussed in detail. The increased cytokine levels in the tumor itself in the DMBA/TPA group can be explained by reference to previous studies indicating that tumorigenesis can be triggered by proinflammatory cytokines (IL-1β, IL-6 and TNF-α), independent of any effects of LEDs or other type of light.

Moreover, topical application of TPA could activate the inflammatory response, which plays an important role in tumorigenesis [32]. Excessive IL-1β, IL-6, and TNF-α levels are associated with exacerbation of various conditions, including skin tumorigenesis [33,34]. TNF-α production was reported to be expressed primarily in the inflammatory response to skin injury [35].

The mechanism underlying the increase in tumor tissue caused by LED treatment should be investigated in future studies. As a result of spectrometer analysis of DMBA, TPA, and acetone that dissolves DMBA and TPA using a (UV-1650, SHIMADZU, Kyoto, Japan), it appears that the photochemical interaction does not occur at red light. This result suggests the increased tumor incidence and proliferation is not caused by photochemical reaction (Suppl. Fig. 4). In addition, as shown in the supplementary Fig. 3, LED is not involved in tumor generation. Therefore, it is speculated that LEDs are involving the tumor proliferation process after tumor initiation by DMBA and TPA application. Such a theory is supported by previous reports showing increased differentiation and proliferation of immature cells which resembles the tumor proliferation model [30]. Also, increases in circulating levels of proinflammatory cytokines could be related to increased tumor size, which would likely have a major impact on homeostasis and the immune response in experimental animals. The difference of species and strains must be considered when transferring the data to clinical issues. According to prior publication, it is suggested that these hair less mouse strains (which include the one used in current study) are very similar to human skin in several ways and do have tendencies to develop skin malignancies by UV exposure like human skin [36]. However, according to several reports, some strains of mice (which might be the background strain of hair less mouse used in this study) are known to be relatively resistant for tumor generation by UV treatment [37,38]. Therefore, in the present study, we have additionally included different strain of mouse (ICR mouse) and showed similar increased proliferation of

Biomedical Optics EXPRESS

tumor compared to control. In addition, in this ICR mouse no tumor development by LED (+ acetone) application was observed. Comparison of light energy power between animal and clinical studies, and calculating the clinical effects modifying the data from current data would be insufficient because there are so many things to consider such as thickness of skin, body weight, and existence of melanocyte, etc.. To unsolved the issue, clinical study, which would not be easy to perform, should be planned to evaluate the safety of LED devices in the possible skin tumor patients.

The results of the present study indicated that LED treatment can promote the development of skin tumors under conditions conducive to tumorigenesis. The mechanism by which LED treatment acts on normal and tumor cells is not fully understood, and the use of LEDs as a treatment modality is still controversial [29]. Before LEDs can be applied with confidence as a therapeutic modality in an oncology setting, it is necessary to investigate the effects and dose-response characteristics of therapy based on LED treatment at a non-clinical level, to definitively determine its safety and efficacy.

Funding. Basic Science Research Program through the National Research Foundation of Korea funded by the Ministry of Education (NRF-2020R1A6A1A03043283), supported by Creative Materials Discovery Program through the National Research Foundation of Korea (NRF) funded by Ministry of Science and ICT, South Korea (NRF-2019M3D1A1078943); National Research Facilities and Equipment Center (NFEC) grant funded by the Korea government (Ministry of Education) (2019R1A6C1010033).

Acknowledgements. This research was supported by Basic Science Research Program through the National Research Foundation of Korea (NRF) funded by the Ministry of Education (NRF-2020R1A6A1A03043283), supported by Creative Materials Discovery Program through the National Research Foundation of Korea (NRF) funded by Ministry of Science and ICT (NRF-2019M3D1A1078943). National Research Facilities & Equipment Center (NFEC) grant funded by the Korea government (Ministry of Education) (No. 2019R1A6C1010033). The English in this document has been checked by at least two professional editors, both native speakers of English.

Disclosures. All Authors of this manuscript declare that there are no conflicts of interest regarding this study.

Data availability. Data underlying the results presented in this paper are not publicly available at this time but may be obtained from the authors upon reasonable request.

Supplemental document. See Supplement 1 for supporting content.

References

1. Y. Y. Huang, K. Nagata, C. E. Tedford, T. McCarthy, and M. R. Hamblin, "Low-level laser therapy (LLLT) reduces oxidative stress in primary cortical neurons in vitro," J. Biophotonics **6**(10), 829–838 (2012).
2. F. Baez and L. R. Reilly, "The use of light-emitting diode therapy in the treatment of photoaged skin," J. Cosmet. Dermatol. **6**(3), 189–194 (2007).
3. D. J. Goldberg, S. Amin, B. A. Russell, R. Phelps, N. Kellett, and L. A. Reilly, "Combined 633-nm and 830-nm led treatment of photoaging skin," J. Drugs Dermatol. **5**(8), 748–753 (2006).
4. S. Y. Lee, K. H. Park, J. W. Choi, J. K. Kwon, D. R. Lee, M. S. Shin, J. S. Lee, C. E. You, and M. Y. Park, "A prospective, randomized, placebo-controlled, double-blinded, and split-face clinical study on LED phototherapy for skin rejuvenation: clinical, profilometric, histologic, ultrastructural, and biochemical evaluations and comparison of three different treatment settings," J. Photochem. Photobiol., B **88**(1), 51–67 (2007).
5. B. A. Russell, N. Kellett, and L. R. Reilly, "A study to determine the efficacy of combination LED light therapy (633 nm and 830 nm) in facial skin rejuvenation," J. Cosmet. Laser Ther. **7**(3-4), 196–200 (2005).
6. R. A. Weiss, D. H. McDaniel, R. G. Geronemus, and M. A. Weiss, "Clinical trial of a novel non-thermal LED array for reversal of photoaging: clinical, histologic, and surface profilometric results," Lasers Surg. Med. **36**(2), 85–91 (2005).
7. R. A. Weiss, M. A. Weiss, R. G. Geronemus, and D. H. McDaniel, "A novel non-thermal non-ablative full panel LED photomodulation device for reversal of photoaging: digital microscopic and clinical results in various skin types," J. Drugs Dermatol. **3**(6), 605–610 (2004).
8. M. W. Berns and J. S. Nelson, "Laser applications in biomedicine. Part I: biophysics, cell biology, and biostimulation," J. Laser Appl. **1**(1), 34–39 (1988).
9. P. E. McGuff, R. A. Deterling Jr., and L. S. Gottlieb, "Laser radiation for metastatic malignant melanoma," JAMA **195**(5), 393–394 (1966).
10. P. E. McGuff, L. S. Gottlieb, I. Katayama, and C. K. Levy, "Comparative study of effects of laser and/or ionizing radiation therapy on experimental or human malignant tumors," AJR, Am. J. Roentgenol. **96**(3), 744–748 (1966).

Biomedical Optics EXPRESS

11. C. M. J. S. de, A. N. Pinheiro, S. C. de Oliveira, G. T. Aciole, J. A. Sousa, M. C. Canguss, and J. N. Dos Santos, "Influence of laser phototherapy (λ660 nm) on the outcome of oral chemical carcinogenesis on the hamster cheek pouch model: histological study," Photomed. Laser Surg. **29**(11), 741–745 (2011).
12. L. Gavish, Y. Asher, Y. Becker, and Y. Kleinman, "Low level laser treatment stimulates mitochondrial membrane potential and disperses subnuclear promyelocytic leukemia protein," Lasers Surg. Med. **35**(5), 369–376 (2004).
13. T. Karu, "Primary and secondary mechanisms of action of visible to near-IR radiation on cells," J. Photochem. Photobiol., B **49**(1), 1–17 (1999).
14. P. M. Elias, "The skin barrier as an innate immune element," Semin. Immunopathol. **29**(1), 3–14 (2007).
15. A. Bashkatov, E. Genina, V. Kochubey, and V. Tuchin, "Optical properties of human skin, subcutaneous and mucous tissues in the wavelength range from 400 to 2000 nm," J. Phys. D: Appl. Phys. **38**(15), 2543–2555 (2005).
16. T. L. Troy and S. N. Thennadil, "Optical properties of human skin in the near infrared wavelength range of 1000 to 2200 nm," J. Biomed. Opt. **6**(2), 167–176 (2001).
17. D. Barolet, C. J. Roberge, F. A. Auger, A. Boucher, and L. Germain, "Regulation of skin collagen metabolism in vitro using a pulsed 660 nm LED light source: clinical correlation with a single-blinded study," J. Invest. Dermatol. **129**(12), 2751–2759 (2009).
18. J. Bhat, J. Birch, C. Whitehurst, and S. W. Lanigan, "A single-blinded randomised controlled study to determine the efficacy of Omnilux Revive facial treatment in skin rejuvenation," Lasers Med. Sci. **20**(1), 6–10 (2005).
19. R. A. Weiss, D. H. McDaniel, R. G. Geronemus, M. A. Weiss, K. L. Beasley, G. M. Munavalli, and S. G. Bellew, "Clinical experience with light-emitting diode (LED) photomodulation," Dermatol. Surg. **31**, 1199–1205 (2006).
20. K. Brown, A. Buchmann, and A. Balmain, "Carcinogen-induced mutations in the mouse c-Ha-ras gene provide evidence of multiple pathways for tumor progression," Proc. Natl. Acad. Sci. U. S. A. **87**(2), 538–542 (1990).
21. T. J. Slaga, "Overview of tumor promotion in animals," Environ. Health Perspect. **50**, 3–14 (1983).
22. T. Niu, Y. Tian, Q. Ren, L. Wei, X. Li, and Q. Cai, "Red light interferes in UVA-induced photoaging of human skin fibroblast cells," Photochem. Photobiol. **90**(6), 1349–1358 (2014).
23. S. Young, P. Bolton, M. Dyson, W. Harvey, and C. Diamantopoulos, "Macrophage responsiveness to light therapy," Lasers Surg. Med. **9**(5), 497–505 (1989).
24. J. H. Tsai, J. L. Donaher, D. A. Murphy, S. Chau, and J. Yang, "Spatiotemporal regulation of epithelial-mesenchymal transition is essential for squamous cell carcinoma metastasis," Cancer Cell **22**(6), 725–736 (2012).
25. C. Frantz, K. M. Stewart, and V. M. Weaver, "The extracellular matrix at a glance," J. Cell Sci. **123**(24), 4195–4200 (2010).
26. N. I. Nissen, M. Karsdal, and N. Willumsen, "Collagens and Cancer associated fibroblasts in the reactive stroma and its relation to Cancer biology," J. Exp. Clin. Cancer Res. **38**(1), 115 (2019).
27. C. Shen, S. Wang, Y. Shan, Z. Liu, F. Fan, L. Tao, Y. Liu, L. Zhou, C. Pei, H. Wu, C. Tian, J. Ruan, W. Chen, A. Wang, S. Zheng, and Y. Lu, "Chemomodulatory efficacy of lycopene on antioxidant enzymes and carcinogen-induced cutaneum carcinoma in mice," Food Funct. **5**(7), 1422–1431 (2014).
28. G. F. Passos, R. Medeiros, R. Marcon, A. F. Nascimento, J. B. Calixto, and L. F. Pianowski, "The role of PKC/ERK1/2 signaling in the anti-inflammatory effect of tetracyclic triterpene euphol on TPA-induced skin inflammation in mice," Eur. J. Pharmacol. **698**(1-3), 413–420 (2013).
29. A. R. Coombe, C. T. Ho, M. A. Darendeliler, N. Hunter, J. R. Philips, C. C. Chapple, and L. W. Yum, "The effects of low level laser treatment on osteoblastic cells," Clin. Orthod Res. **4**(1), 3–14 (2001).
30. M. Kreisler, H. Al Haj, and B. D'Hoedt, "Temperature changes induced by 809-nm GaAlAs laser at the implant-bone interface during simulated surface decontamination," Clin. Oral Implants Res. **14**(1), 91–96 (2003).
31. C. E. Werneck, A. L. Pinheiro, M. T. Pacheco, C. P. Soares, and J. L. de Castro, "Laser light is capable of inducing proliferation of carcinoma cells in culture: a spectroscopic in vitro study," Photomed. Laser Surg. **23**(3), 300–303 (2005).
32. S. C. Chaudhary, M. S. Siddiqui, M. Athar, and M. S. Alam, "Geraniol inhibits murine skin tumorigenesis by modulating COX-2 expression, Ras-ERK1/2 signaling pathway and apoptosis," J. Appl. Toxicol. **33**(8), 828–837 (2013).
33. D. D. Lofrumento, G. Nicolardi, A. Cianciulli, F. De Nuccio, V. La Pesa, V. Carofiglio, T. Dragone, R. Calvello, and M. A. Panaro, "Neuroprotective effects of resveratrol in an MPTP mouse model of Parkinson's-like disease: possible role of SOCS-1 in reducing pro-inflammatory responses," Innate Immun. **20**(3), 249–260 (2014).
34. C. Ma, L. Hu, G. Tao, W. Lv, and H. Wang, "An UPLC-MS-based metabolomics investigation on the anti-fatigue effect of salidroside in mice," J. Pharm. Biomed. Anal. **105**, 84–90 (2015).
35. H. Choi, H. N. Nguyen, and F. S. Lamb, "Inhibition of endocytosis exacerbates TNF-α-induced endothelial dysfunction via enhanced JNK and p38 activation," Am. J. Physiol. Heart Circ Physiol. **306**(8), H1154–H1163 (2014).
36. A. Y. Voigt, M. Michaud, K. Y. Tsai, J. Oh, and J. P. Sundberg, "Differential hairless mouse strain-specific susceptibility to skin cancer and sunburn," J. Invest. Dermatol. **139**(8), 1837–1840.e3 (2019).
37. T. Kitajima, M. Iwashiro, K. Kuribayashi, and S. Imamura, "Effect of parent genetic background on latency and antigenicity of UV-induced tumors originating in F1 hybrids," Exp. Dermatol. **4**(1), 42–45 (1995).
38. M. Naito and J. DiGiovanni, "Genetic background and development of skin tumors," Carcinog. Compr. Surv. **11**, 187–212 (1989).